

Tying knots in particle physics

Minoru Eto,^{1,2,3} Yu Hamada,^{4,2} and Muneto Nitta^{5,2,3}

¹*Department of Physics, Yamagata University, Kojirakawa-machi 1-4-12, Yamagata, Yamagata 990-8560, Japan*

²*Research and Education Center for Natural Sciences, Keio University,*

4-1-1 Hiyoshi, Yokohama, Kanagawa 223-8521, Japan

³*International Institute for Sustainability with Knotted Chiral Meta Matter(SKCM²), Hiroshima University, 1-3-2 Kagamiyama, Higashi-Hiroshima, Hiroshima 739-8511, Japan*

⁴*Deutsches Elektronen-Synchrotron DESY, Notkestr. 85, 22607 Hamburg, Germany*

⁵*Department of Physics, Keio University, 4-1-1 Hiyoshi, Kanagawa 223-8521, Japan*

Lord Kelvin’s pioneering hypothesis that the identity of atoms is knots of vortices of the aether had a profound impact on the fields of mathematics and physics despite being subsequently refuted by experiments. While knot-like excitations emerge in various systems of condensed matter physics, the fundamental constituents of matter have been revealed to be elementary particles such as electrons and quarks, seemingly leaving no room for the appearance of knots in particle physics. Here, we show that knots indeed appear as meta-stable solitons in a realistic extension of the standard model of particle physics that provides the QCD axion and right-handed neutrinos. This result suggests that during the early Universe, a “knot dominated era” may have existed, where knots were a dominant component of the Universe, and this scenario can be tested through gravitational wave observations. Furthermore, we propose that the end of this era involves the collapse of the knots via quantum tunneling, leading to the generation of matter-antimatter asymmetry in the Universe. Our findings exhibit the significant role of knots in particle physics and represent a modern version of Kelvin’s hypothesis.

INTRODUCTION

Knots, mathematically defined as closed curves embedded into three-dimensional space, appear not only when tying a tie but also in various scientific fields today, as pioneered by William Thomson, also known as Lord Kelvin. He conjectured that atoms, thought of as fundamental building blocks of matter at that time, are made from knots of vortices of the aether, which means that knots are the ultimate origins of all matter in our Universe [1]. Although this elegant conjecture had attracted much attention from many physicists and mathematicians, it was eventually falsified by Michelson and Morley’s experiment ruling out the existence of aether, leading to the development of knot theory [2] as a separate mathematical discipline.

Even though Kelvin’s idea failed to explain the most fundamental aspects of nature, the concept of knots has found extensive applications in various domains. One of the characteristics of knots is their topological nature; knots do not disappear unless the strings break or intersect, which has played a crucial role in persistent phenomena [3]. For instance, knots appear as vortex knots or topological solitons called Hopfions [4] in diverse subjects such as fluid dynamics [5–9], superconductors [10, 11], Bose-Einstein condensates [12–16], ³He superfluids [17, 18], nematic liquid crystals [19–28], colloids, magnets [29], optics [30], electromagnetism [31–34], and active matter [35]. The stability of the solitons is ensured by the topological invariant associated with knots.

In modern physics, the understanding of the fundamental nature of matter has progressed from atoms to nucleons and ultimately to quarks and gluons primarily through elementary particle physics, instead of knots.

Here a natural question may arise: Are knots truly irrelevant within the realm of elementary particle physics? It is known that a knot invariant in mathematics arises from topological field theories known as the Chern-Simons theory [36], which exhibits a direct connection between theoretical physics and mathematics. In addition, a knot as a soliton is proposed [4, 37–41] in a field-theoretic toy model called the Faddeev-Skyrme model, in which the stability of the knot soliton requires non-renormalizable interactions destroying the predictability of the model. Nevertheless, knots have received relatively less attention compared to condensed matter physics and other fields. In particular, knots have never appeared in phenomenologically viable models in the context of particle physics.

Here we revisit Kelvin’s idea in elementary particle physics. We theoretically show the existence of stable knot solitons in a particle physics model for the first time. The model is a simple setup containing global and local $U(1)$ symmetries denoted by $U(1)_{\text{global}}$ and $U(1)_{\text{local}}$, respectively. The two symmetries are spontaneously broken by condensations of two complex scalar fields, and thus a superfluid and superconductor are simultaneously realized, resulting in the production of two kinds of string-like defects called flux tubes and superfluid vortices, respectively. String loops (either knots or unknots) made of the single species of the flux tube or superfluid vortex shrink due to their tensions and eventually disappear [12, 13]. In contrast, it turns out that the knot solitons made by linking the two types of the strings remain stable. Such configurations are known as two-component links in knot theory. The stability is realized by the so-called Chern-Simons coupling between the Nambu-Goldstone (NG) boson and the massive $U(1)_{\text{local}}$

gauge field. The gradient of the NG field and the magnetic flux of the gauge field induce a $U(1)_{\text{local}}$ electric charge and hence electric flux around the string loop.¹

By identifying the $U(1)_{\text{global}}$ and $U(1)_{\text{local}}$ symmetries with the $U(1)$ Peccei-Quinn symmetry [45, 46] and $U(1) B - L$ (baryon number minus lepton number) symmetry, which are popular hypothetical symmetries to resolve mysteries unanswered by the Standard Model (SM) of particle physics, our setup becomes a realistic model as a microscopic theory beyond the SM. In addition, we below argue a cosmological scenario that the knot solitons were produced at the early stage of the Universe. Because they can be sufficiently abundant to dominate the energy density of the Universe, this scenario is testable in terms of stochastic signals of gravitational waves. Furthermore, the knots eventually decay by a quantum effect, and the decay can produce an imbalance between matter and antimatter, which explains why matter is dominant compared to antimatter in the present Universe, see Fig. 1. Thus, this scenario is a modern revival of Kelvin's dream; The Universe was full of knots, and matter originated from them.

THE MODEL

We start with a model that includes two complex scalar fields ϕ_1 and ϕ_2 and a $U(1)$ gauge field. The Lagrangian for the scalars is given as

$$\mathcal{L}_\phi = |D_\mu \phi_1|^2 + |D_\mu \phi_2|^2 - V(\phi_1, \phi_2) \quad (1)$$

with the potential term²

$$V = \lambda(|\phi_1|^2 + |\phi_2|^2 - m^2)^2 - \kappa|\phi_1|^2|\phi_2|^2, \quad (2)$$

and $\lambda, \kappa > 0$. The Lagrangian is invariant under each $U(1)$ phase rotation of the scalars ϕ_1 and ϕ_2 , which we denote $U(1)_1$ and $U(1)_2$, respectively. The covariant derivative is given as $D_\mu \phi_{1(2)} \equiv (\partial_\mu - iq_{1(2)}gA_\mu)\phi_{1(2)}$, where A_μ is the $U(1)$ gauge field and g is its coupling constant. q_1 and q_2 denote $U(1)$ gauge charges of ϕ_1 and ϕ_2 , respectively. For simplicity, we take $q_1 = 1$ and $q_2 = 0$ for the moment, leading to that $U(1)_1$ is promoted to a gauge symmetry called $U(1)_{\text{local}}$ while $U(1)_2$ is a global symmetry denoted by $U(1)_{\text{global}}$. The Lagrangian for the kinetic term of A_μ is given as $\mathcal{L}_g = (-1/4)F_{\mu\nu}F^{\mu\nu}$ with $F_{\mu\nu}$ being the field strength. Thus the full Lagrangian is given as $\mathcal{L} = \mathcal{L}_\phi + \mathcal{L}_g$.

Because of the tachyonic mass parameter $-\lambda m^2 < 0$ in V , the two scalars condense and develop vacuum expectation values (VEVs) as $\langle \phi_1 \rangle = \langle \phi_2 \rangle = v/\sqrt{2}$, which spontaneously break both of the $U(1)_{\text{local}}$ and $U(1)_{\text{global}}$ symmetries.

At the broken phase, quantum corrections can induce the so-called Chern-Simons coupling in addition to the Lagrangian $\mathcal{L}_\phi + \mathcal{L}_g$, which characterizes the coupling between the NG boson $a \equiv -i \arg \phi_2$ and A_μ , given as

$$\mathcal{L}_{\text{CS}} = C a F_{\mu\nu} \tilde{F}^{\mu\nu}, \quad (3)$$

where $\tilde{F}^{\mu\nu} = \epsilon^{\mu\nu\lambda\rho} F_{\lambda\rho}$ and C is a model-dependent dimensionless constant; for instance, it may be induced by one-loop effects of fermions.³ To consider general setups, C is taken as a free parameter in this paper. The model $\mathcal{L}_\phi + \mathcal{L}_g + \mathcal{L}_{\text{CS}}$ includes the axion electrodynamics [51], which has been recently applied in condensed matter physics to describe topological superconductors [52–54].

The spontaneous breaking of the two symmetries $U(1)_{\text{local}}$ and $U(1)_{\text{global}}$ (or, $U(1)_1$ and $U(1)_2$) gives rise to two kinds of vortex strings as topological defects. We call these two strings the ϕ_1 and ϕ_2 strings; for the ϕ_1 string, the phase of ϕ_1 winds around the defect while for the ϕ_2 string the phase of ϕ_2 winds, both of whose windings are topologically protected. Since the ϕ_1 string is a local string, it contains a magnetic flux associated with A_μ , $|\Phi_A| = 2\pi/g$, like flux tubes in superconductors while the ϕ_2 string is a global string without magnetic fluxes like superfluid vortices.

KNOT SOLITON

The Chern-Simons coupling (3) does not affect the individual ϕ_1 or ϕ_2 string because the ϕ_1 (ϕ_2) string does not contain excitation of the NG boson a (the gauge field A_μ), resulting in that (3) vanishes. Thus a loop made of either the ϕ_1 or ϕ_2 string is not stable but shrinks due to their tension and eventually disappears.

Now, make the ϕ_1 and ϕ_2 strings linked. Particularly, one simple example is a link made of a single ϕ_2 string and multiple ϕ_1 strings (See the left panel of Fig. 2). Now the coupling (3) plays a crucial role; it induces the electric flux of the A_μ field around the ϕ_1 string. To see this, let us rewrite the Chern-Simons coupling as

$$\mathcal{L}_{\text{CS}} = -CA^0 \left(\vec{\nabla} a \cdot \vec{B} \right), \quad (4)$$

where \vec{B} is the magnetic field of A_μ , $\vec{B} = \nabla \times \vec{A}$, and we have used that all fields are static. Eq. (4) changes

¹ Note that the stability mechanism by the Chern-Simon coupling is crucial, although knots were discussed in similar systems without such a coupling: liquid metallic hydrogen [42, 43] and the coexistence of a neutron superfluid and a proton superconductor inside neutron star interior [44].

² We here assume an exchange symmetry between the two scalars in the potential for simplicity. This is however not necessary in the following argument; we may add other terms such as $|\phi_2|^4$.

³ If we assume the existence of a UV theory for our model, the coupling C is quantized as $C = Ng^2/32\pi^2$ with an integer N . In such a case, this model possesses an emergent symmetry at low energy, characterized by a mathematical structure called the 4-group [47, 48] while it is the 3-group in the unbroken phase of the $U(1)_{\text{local}}$ symmetry [49, 50].

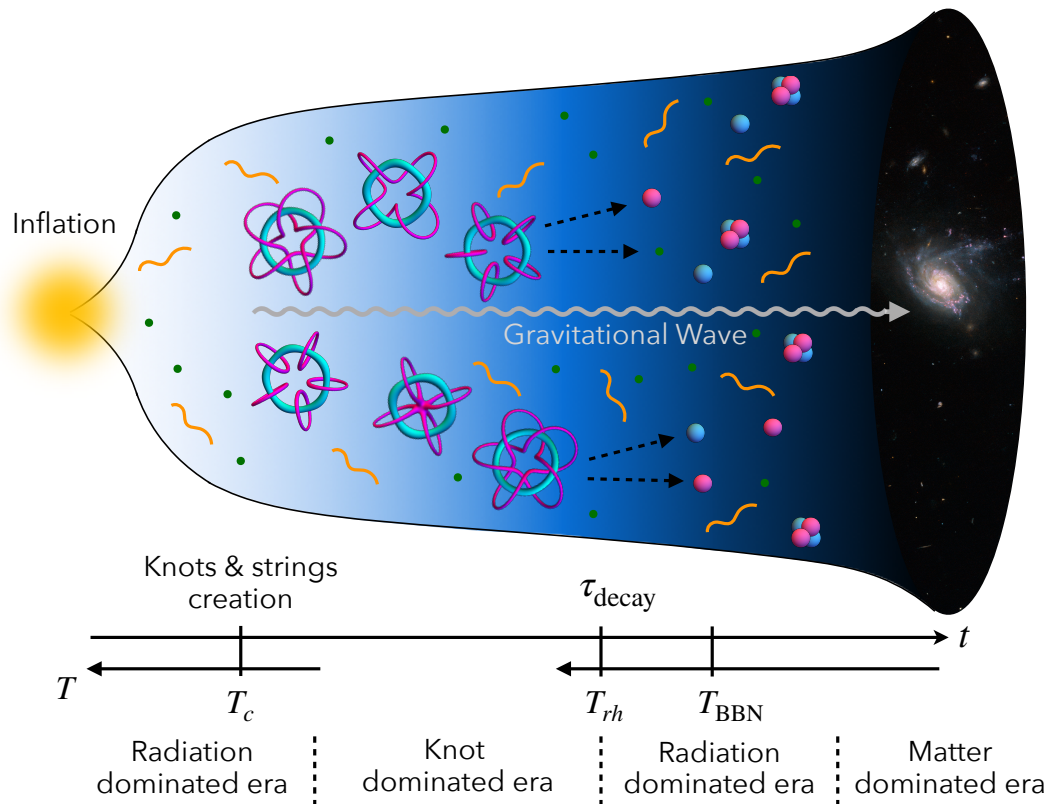


FIG. 1: Illustration of cosmic history in our scenario. After creation of the strings and knots, the knots eventually dominate the energy density of the Universe (knot dominated era). At $t \sim \tau_{\text{decay}}$, they decay into light particles, leading to radiation dominated era again. This decay can produce the correct baryon asymmetry in the Universe via the non-thermal leptogenesis. In addition, the existence of the knot domination is imprinted on stochastic GW spectrum radiated from the string network, which can be tested by future GW observations.

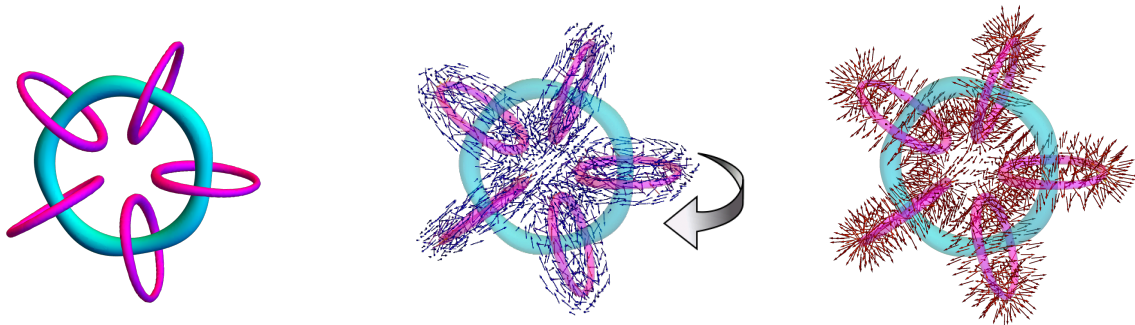


FIG. 2: 3D plots of numerical solution for a knot soliton. The magenta and cyan regions represent the cores of the ϕ_1 and ϕ_2 strings ($|\phi_1|^2/v^2 < 0.1$ and $|\phi_2|^2/v^2 < 0.1$). The single ϕ_2 string loop is linked with five ϕ_1 string loops, so that the solution has the linking number 5. In the middle and right panels, the arrows that are overlaid with transparent string cores indicate the magnetic flux \vec{B} and the electric flux \vec{E} of the massive gauge field A_μ , respectively, and their colors correspond to their strength $|\vec{B}|$ and $|\vec{E}|$. The magnetic flux is along the ϕ_1 strings, one of whose direction is indicated by the large gray arrow, while the electric one comes out from the strings, which means that the strings have net electric charges. We here take $\lambda/g^2 = 10^3$, $\kappa/g^2 = 0.0008$, and $C = 400$. The energy of the solution is $7.0 \times 10^3 v/g$.

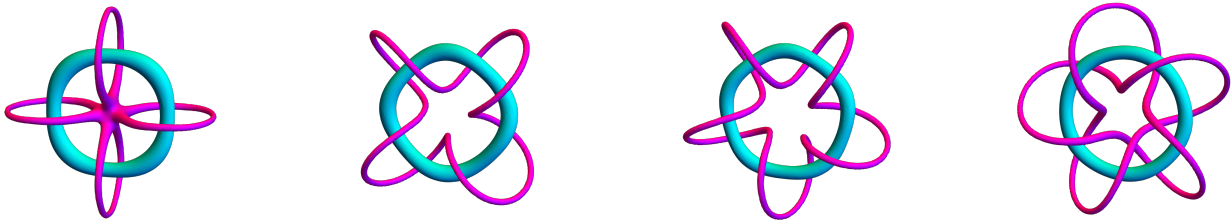


FIG. 3: 3D plots of numerical solutions for other knot solitons. The colors and the parameters are the same as those in Fig. 2. The two left plots have the same linking number 4 and the other plots have the linking number 5. The energy of the solutions are $6.0 \times 10^3 v/g$, $6.3 \times 10^3 v/g$, $7.3 \times 10^3 v/g$ and $7.5 \times 10^3 v/g$ (from left to right).

the Gauss law in the Maxwell equation with respect to A_0 and hence $C \vec{\nabla} a \cdot \vec{B}$ behaves as a source of the electric field.⁴ The total electric charge is estimated to be $C \int d^3x \vec{\nabla} a \cdot \vec{B} = 4\pi^2 C N_{\text{link}}/g$ where the strings are assumed to be sufficiently thin [57]. The integer N_{link} is the linking number of the ϕ_1 and the ϕ_2 strings.⁵ From this, the ϕ_1 strings linking with the ϕ_2 strings get the electric charge, which gives rise to the electric field \vec{E} around the strings. Even though this electric field is screened due to the VEV of ϕ_1 like Meissner effect, for large enough C , the ϕ_1 string loops are prevented from shrinking by the electric field and is stabilized.⁶

In order for the linked configuration to be stable under arbitrary perturbations, another condition $\lambda \gg g^2, \kappa$ is necessary. If this is met, the link of the ϕ_1 and ϕ_2 strings cannot be de-linked, i.e., the strings cannot pass through each other. This is because in the limit of $\lambda \rightarrow \infty$, the linking number is equivalent to the Skyrme number [67, 68] which is characterized by the homotopy group $\pi_3(S^3) \simeq \mathbb{Z}$ defined by a map from S^3 , obtained by a compactification of the real space \mathbb{R}^3 , to S^3 defined by $|\phi_1|^2 + |\phi_2|^2 = \text{const.}$, and hence in this regime, this number approximately becomes a topological invariant.⁷ In practical cases with finite λ , the ϕ_1 and ϕ_2 strings are repelled from each other [11, 72] as far as the condition $\lambda \gg g^2, \kappa$ is met, and hence they cannot be overlapped.

We numerically solve the classical equations of motion (EOMs) to confirm the existence of the stable knot soliton in the model. We perform a minimization procedure for the energy of the configuration starting from

an appropriate initial configuration with the Gauss-law constraint. See Appendix A for the details. After the minimization converges with desired accuracy, the configuration is regarded as the static solution of the EOMs. Fig. 2 shows the cores of the strings of the obtained solution, in which the magenta and cyan colors represent regions $|\phi_1/v|^2 < 0.1$ and $|\phi_2/v|^2 < 0.1$, respectively. We here take $\lambda/g^2 = 10^3$, $\kappa/g^2 = 0.0008$, and $C = 400$. The magnetic and electric fields are also shown by arrows. In this figure, the single ϕ_2 string loop is linked with five ϕ_1 string loops (with the same linking direction), so that the solution has the linking number 5. One can also see that the magnetic flux is along the ϕ_1 strings, one of whose direction is indicated by the large gray arrow. On the other hand, the electric one comes out from the strings, which means that the strings have net electric charges. This is consistent with the argument above.⁸

Note that a similar solution is obtained by acting parity transformation on the knot soliton shown here. This solution has the opposite linking direction of the ϕ_1 and ϕ_2 strings compared to the knot soliton, so that we call this the anti-knot soliton. The anti-knot one has the $U(1)_X$ electric charge (and Skyrme number) with the opposite signs to those of the knot one.

We can also obtain other knot solitons, which are shown in Fig. 3. The leftmost panel shows a single loop of the ϕ_2 string linking with four ϕ_1 string loops. In the other panels, single ϕ_1 and ϕ_2 loops make higher linking number by linking multiple times. The colors are the same as those in Fig. 2. For both types, the energy grows as the linking number gets higher because the electric charge contained in the ϕ_1 string becomes larger. The

⁴ A similar effect is well known for Chern-Simons vortices in 2+1 dimensions [55, 56].

⁵ Formally this is the same as cross helicity in magnetohydrodynamics when we regard $\vec{\nabla} a$ as the velocity of fluid [57, 58].

⁶ A similar vortex loop with the electric charge/current is known as the vorton [59, 60]. The classical and quantum studies of the stability of vortons are given in Refs. [39, 61–66]. Our knot soliton considered here is however different from those in the sense that it does not contain internal degrees of freedom on the loop.

⁷ This is similar to the case of Skyrmions in two-component Bose-Einstein condensates [69–71].

⁸ It is known that the electric flux may cause an instability for the NG boson and gauge field due to the Chern-Simons coupling [73]. Even though our setup has some differences from theirs, such as the mass of the gauge field, this effect still exists in our case. Consequently, the NG boson a and gauge field A_i exhibit oscillating profiles inside the ϕ_1 strings. However, profiles inside the strings are not crucial for the stability because the amount of the electric charge is fixed by the linking number unless the strings do not have overlap.

energy of all configurations are almost dominated by the ϕ_1 strings and the electric flux. Within the same linking number, the energy gets larger as the length of the ϕ_1 string gets longer. Therefore, the leftmost solution in Fig. 3 and that in Fig. 2 have the least energy with the linking number 4 and 5, respectively. Although we did not find any more other knot solitons with our numerical code, this does not necessarily mean non-existence of other solitons.

Even when the (anti-)knot solitons are classically stable, they can decay due to quantum tunneling, whose lifetime is denoted by τ_{decay} . One possible decay process is the de-linking process, i.e., the ϕ_1 and ϕ_2 strings pass through each other by quantum tunneling. The calculation of the decay rate is complicated and beyond the scope of this paper. Instead, we will later relate the decay rate to the cosmological history of the knot solitons.

PARTICLE PHENOMENOLOGY

In spite of the great success of the SM, there are still several problems that the SM is not able to answer, such as dark matter of the Universe, tiny masses of the neutrinos, strong CP problem, and baryon asymmetry in the Universe. (For a review, see, e.g., Ref. [74].) It is believed that (some of) these problems should be resolved by new physics beyond the SM.

Particularly, one elegant way to extend the SM is to introduce new symmetries that do not exist within the SM. The strong CP problem and dark matter are simultaneously explained by introducing a global $U(1)$ symmetry called the Peccei-Quinn symmetry [45, 46] (denoted by $U(1)_{\text{PQ}}$), which spontaneously breaks and provides a NG boson, the QCD axion [75, 76]. In addition, it is well motivated to introduce the gauge $B-L$ (baryon number minus lepton number) symmetry, $U(1)_{B-L}$,⁹ because it requires the existence of the right-handed neutrinos and its spontaneous breaking gives them Majorana masses, which naturally explain the tiny neutrino masses in terms of the type-I seesaw mechanism [77–80]. The right-handed neutrinos are also expected to play key roles to generate baryon asymmetry in the Universe. Furthermore, the $U(1)_{B-L}$ gauge symmetry naturally arises from grand unified theories (GUTs).

Now we apply our study on the knot soliton to particle physics models and discuss its influence on cosmology. One realistic and promising setup is obtained by identifying the $U(1)_{\text{local}}$ and $U(1)_{\text{global}}$ symmetries in (1) as the $U(1)_{B-L}$ and $U(1)_{\text{PQ}}$ symmetries, respectively. In order for ϕ_1 to couple with right-handed neutrinos, the $B-L$ charge of ϕ_1 is taken as $q_1 = 2$ instead of 1 while keeping $q_2 = 0$. We emphasize that

⁹ The SM contains *global* $U(1)_{B-L}$ symmetry as an accidental symmetry although it cannot be gauged due to the gauge anomaly in the SM unless right-handed neutrinos are introduced.

this setup is well motivated because it can elegantly resolve some of the mysteries in particle physics as stated above.¹⁰ In this setup, the QCD axion is identified with the phase of ϕ_2 . For this to solve the strong CP problem, we need additional fermionic fields inducing the Chern-Simons coupling between the QCD axion and gluon, which may be realized by introducing Kim-Shifman-Vainshtein-Zakharov(KSVZ)-like [83, 84] heavy quarks. How the QCD axion couples to the $B-L$ and SM gauge bosons depends on the charge assignment of the fermionic sectors, which is kept as general as possible hereafter. From the astrophysical constraints on the QCD axion, we take $v \gtrsim 10^8$ GeV [85–88].

COSMOLOGY AND GRAVITATIONAL WAVE

Now let us discuss cosmological fate of the knot solitons. The Universe was very hot and full of thermal relativistic particles at early stages (after the cosmic inflation). When the temperature T of the Universe is much larger than v , the $U(1)_{B-L}$ and $U(1)_{\text{PQ}}$ symmetries are not broken while they get spontaneously broken almost simultaneously due to a phase transition when T gets less than a critical temperature $T_c \simeq v$. At the transition, the ϕ_1 and ϕ_2 strings are produced by the Kibble-Zurek mechanism [89, 90]. The produced strings have completely random configurations, in which some of the strings are linked with finite probability. After the oscillation and the random motion are relaxed, long ϕ_1 and ϕ_2 strings form conventional networks whose typical length scale is the Hubble scale. Besides them, small loops with the linking configurations become the knot solitons that we have studied above. In Ref. [91], the linking number density of a single species of string formed during a phase transition is given as $10^{-4}\xi^{-3}$, where ξ is the correlation length to be $\xi \sim T_c^{-1}$. Thus we use this value as a reference value for the number density of the (anti-)knot solitons: $n_{\text{knot}}(T = T_c) \sim 10^{-4}\xi^{-3}$.¹¹

After the production, the knot solitons behave as heavy particles decoupled from the thermal bath with the long lifetime τ_{decay} , and hence their energy density is given as $\rho_{\text{knot}} = M n_{\text{knot}}$ with the mass of the knots $M \simeq \mathcal{O}(10^3) v/g$. Since ρ_{knot} is diluted by the cosmic expansion being proportional to the cubic of the scale factor $a(t)^{-3}$, which is slow compared to the radiation energy density in the thermal plasma, $\rho_{\text{rad}} \propto a(t)^{-4}$, the energy density of the knots eventually overcomes the latter and

¹⁰ When one allows ϕ_2 to have a small non-zero charge under $U(1)_{B-L}$ and introduces fermionic matters charged under the $U(1)_{B-L}$ and $U(1)_{\text{PQ}}$ symmetries, the setup may have a bonus [81, 82] that the quality of the $U(1)_{\text{PQ}}$ symmetry is protected against the effect of quantum gravity. (See Refs. [81, 82] for more details.)

¹¹ Note that results given below do not depend on the value of the produced number density $n_{\text{knot}}(T_c)$ as long as they dominate the energy density of the Universe before they decay.

dominates the total energy density of the Universe when the temperature reaches $T \sim M n_{\text{knot}}(T_c)/(g_* T_c^3)$. Here g_* is the number of the degrees of freedom for relativistic particles, $g_* = \mathcal{O}(10^2)$. Note that this domination persists until they decay. We call this epoch “knot dominated era”. When cosmic time exceeds the lifetime of the knots, $t \sim \tau_{\text{decay}}$, they decay by the quantum tunneling releasing their energy into light particles, which leads to the radiation dominated epoch again via a secondary reheating. Assuming instantaneous decays, the temperature of the reheated thermal bath is found to be [92]

$$T_{rh} \simeq \left(\frac{30}{\pi^2 g_*} \frac{3M_{\text{pl}}^2}{8\pi} \Gamma^2 \right)^{1/4}. \quad (5)$$

with $\Gamma \equiv 1/\tau_{\text{decay}}$ and M_{pl} being the decay rate and the Planck mass, respectively. Note that Γ is typically exponentially suppressed because of non-perturbative processes. In order to realize the successful Big-Bang Nucleosynthesis (BBN), T_{rh} must be larger than $\mathcal{O}(1)$ MeV [93–95]. Therefore, the Universe experiences the knot dominated era sandwiched by two radiation dominated eras before BBN. See Fig. 1.

Remarkably, this existence of the knot dominated era can be observed in terms of gravitational waves (GW) when there exists a sufficient GW source. Fortunately, this model already contains a possible source of GW: the string network. Thermal history of the Universe including the knot dominated era is imprinted on the GW spectrum. Following the study given in Refs. [96–98], we obtain an expected spectrum of the stochastic GW emitted from the network of the ϕ_1 strings depending on v and T_{rh} as shown in Fig. 4. Here $\Omega_{\text{GW}} h^2$ is defined as $\Omega_{\text{GW}} h^2 = (d\rho_{\text{GW}}(f)/d \log f) h^2 / \rho_c$ with h being the dimensionless Hubble constant, $\rho_{\text{GW}}(f)$ the GW energy density for a frequency f observed today, and ρ_c the critical energy density. We also show in Fig. 4 the observed signals of NANOGrav 15-year data set [99] as gray region¹² and projected sensitivity curves of future GW observatories. The data points of the projected sensitivity curves are taken from Ref. [101]. One can see that the spectra are deviated due to the existence of the knot dominated era (solid lines) and can be distinguished from the conventional spectra without the knot domination (red dashed lines).

BARYOGENESIS

Our Universe is baryon asymmetric, i.e., baryon is more than anti-baryon as characterized by a quantity

¹² We do not aim to explain the NANOGrav 15-yrs signals by the GW spectrum from the ϕ_1 strings because the signals are unlikely to be explained by cosmic strings alone [100]. Instead they may be explained by combining the spectrum of the strings with those of super massive black holes.

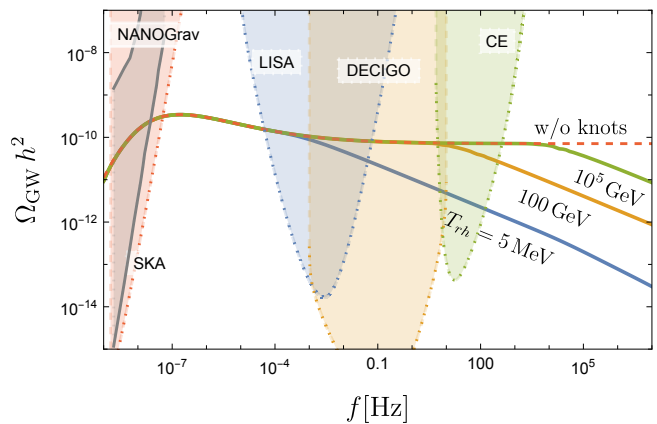


FIG. 4: Stochastic GW spectrum $\Omega_{\text{GW}} h^2$ from the network of the ϕ_1 strings with $G\mu = 10^{-11}$, in which G and μ are the Newton constant and the ϕ_1 string tension given as $\mu \simeq v^2$. The red dashed line corresponds to the cosmological evolution without the knot solitons while the solid ones include the knot dominated era with different reheating temperatures due to the knot decay, $T_{rh} = 5$ MeV (blue), 100 GeV (orange), and 10^5 GeV (green). We also show the observed signals of NANOGrav 15-year data set [99] as gray region and projected sensitivity curves of future observatories: DECIGO [102] (orange), Cosmic Explorer (CE) [103] (green), LISA [104] (blue), and Square Kilometer Array (SKA) [105] (red).

$Y_B \equiv (n_B - n_{\bar{B}})/s \simeq 0.8 \times 10^{-10}$ [74, 106] where $n_B(\bar{B})$ and s are the number density of (anti)baryon and the entropy density, respectively. The SM however cannot explain this asymmetry. As stated above, the knot solitons remain in the Universe and later decay into particles. When T_{rh} is larger than the electroweak (EW) scale $\mathcal{O}(10^2)$ GeV,¹³ this decay process can produce baryon asymmetry in the Universe in a similar way to non-thermal leptogenesis via inflaton decay [107–111]. Note that the baryon asymmetry produced at earlier stages than the end of the knot domination is diluted by the secondary reheating due to the knot decay. For simplicity, we here assume it to be sufficiently diluted away and concentrate on the baryon asymmetry produced by the knot decay.

To see that this scenario works, we should note that to ensure cancellation of the gauge anomaly of $U(1)_{B-L}$, this model contains the right-handed (RH) neutrinos ν_R described by the Lagrangian

$$\mathcal{L}_R = i\bar{\nu}_{Ri} \not{\partial} \nu_{Ri} + \left(y_R^{ij} \phi_1^* \nu_{Ri}^\dagger \nu_{Rj}^c + y_D^{ij} \bar{\nu}_{Ri} H^\dagger \ell_j + \text{h.c.} \right), \quad (6)$$

¹³ There can be an alternative scenario of baryogenesis even when T_{rh} is smaller than the electroweak scale. This is complementary to the scenario presented here. See Appendix C for the details.

where H and ℓ are the SM Higgs doublet and lepton doublet, respectively. y_R^{ij} (y_D^{ij}) is the Majorana-type (Dirac-type) Yukawa coupling constant. The indices i, j denote the generations and run as $i, j = 1, 2, 3$. After ϕ_1 takes the VEV v , the RH neutrinos get Majorana masses, whose mass eigenvalues and eigenstates are denoted by M_{Ri} and N_i , respectively. We suppose $M_{R1} < M_{R2} < M_{R3}$, so that the baryon asymmetry is dominantly produced via the lightest state N_1 . Through the couplings with ϕ_1 and A_μ in \mathcal{L}_R , the decay of a knot soliton produces N_i . We parameterize an energy fraction of the produced N_1 compared to the knot static energy as $f_{N_1} \in [0, 1]$, i.e., the produced number of N_1 is given as $f_{N_1} M/M_{R1}$, in which f_{N_1} is not expected to be very small when M_{R1} is smaller than the gauge boson mass.

Typically N_1 has much larger decay rate, whose main decay channels are $N_1 \rightarrow H + \ell$ and $N_1 \rightarrow H^\dagger + \bar{\ell}$, than that of the knot soliton, so that the produced N_1 immediately decay into H (H^\dagger) and ℓ ($\bar{\ell}$). When their decay rates are different, the lepton asymmetry $n_L - n_{\bar{L}}$ can be produced. See Appendix B for the calculation of the lepton asymmetry. Through the EW sphaleron process as usual, some of the lepton asymmetry is converted into the baryon asymmetry. Thus leptogenesis is followed by baryogenesis.

When the masses M_{R1}, M_{R2}, M_{R3} are not degenerated, the produced baryon asymmetry is maximized for a hierarchical case $M_{R1} \ll M_{R2}, M_{R3}$ [112–115], leading to

$$Y_B \simeq 4.1 \times 10^{-11} f_{N_1} \left(\frac{T_{rh}}{10^6 \text{ GeV}} \right) \left(\frac{m_3}{0.05 \text{ eV}} \right) \delta_{\text{eff}}, \quad (7)$$

where m_3 and δ_{eff} are the heaviest mass of the active neutrinos and the effective CP phase coming from the Yukawa matrices, respectively. If one takes $f_N = \delta_{\text{eff}} = \mathcal{O}(1)$, the correct baryon asymmetry can be explained for $T_{rh} \simeq 10^6 \text{ GeV}$. This case is however difficult to test in terms of GW spectrum by near future experiments because it requires sensitivity for higher frequency region than 10^5 Hz as shown in Fig. 4.

On the other hand, when the masses of N_1 and N_2 are almost degenerated, Y_B can be enhanced to be as large as

$$Y_B \simeq 0.8 \times f_{N_1} \frac{T_{rh}}{M_{R1}} \quad (8)$$

like resonant leptogenesis [116, 117]. In such a case, the reheating temperature T_{rh} can be lowered to, say, $\mathcal{O}(10^2) \text{ GeV}$ for $M_{R1} = 10^{12} \text{ GeV}$. This case is quite attractive because the stochastic GW spectrum lies within the range of CE, and hence this scenario is expected to be tested. (See the orange line in Fig. 4.)

To summarize, within reasonable setups, the decay of the knot solitons can produce the correct baryon asymmetry, which gives the matter-antimatter asymmetry in the present Universe. In this sense, although the knot itself is not the building block of matter as conjectured by Kelvin, it might be the origin of matter and a key ingredient of nature. Fig. 1 shows the summary of cosmological history.

For further studies in the phenomenological perspective, we need concrete model building. Particularly, it is worth considering embedding this setup into GUTs such as $SO(10)$ GUTs since $U(1)_{B-L}$ and the SM gauge group are elegantly embedded into $SO(10)$ as is well-known. Although we have taken C , the coefficient of the Chern-Simons coupling, as a free parameter, it may be explained as one-loop effect of matter fermions charged under the $U(1)_{B-L}$ and $U(1)_{\text{PQ}}$ symmetries. It is not obvious whether the parameter space and field contents that ensure the existence of the knot soliton is compatible with GUTs. If so, the knot soliton can be regarded as an indirect probe of GUTs. In any case, the knot soliton in particle physics has many potential applications to understand fundamental aspects of nature.

ACKNOWLEDGMENTS

The authors would like to thank Simone Blasi, Asuka Ito, Ryusuke Jinno, Kohei Kamada, Yuka Kotorii, Shunya Mizoguchi, Nobuyuki Matsumoto, Hiroto Shibuya, Fumio Uchida, Wen Yin and Ryo Yokokura for useful comments. The numerical calculations were carried out on Yukawa-21 at YITP in Kyoto University. This work is supported in part by JSPS Grant-in-Aid for Scientific Research KAKENHI Grant No. JP22H01221 (M. E. and M. N.) and No. JP22KJ3123 (Y. H.) and by the Deutsche Forschungsgemeinschaft under Germany's Excellence Strategy - EXC 2121 Quantum Universe - 390833306. The work of M. N. is supported in part by the WPI program ‘‘Sustainability with Knotted Chiral Meta Matter (SKCM²)’’ at Hiroshima University. The photo of a galaxy used in Fig. 1 is taken from NASA Image and Video Library.

APPENDIX

A. Numerical technique to obtain knot solitons

We give numerical technique performed in this work. Because we are interested in static solutions of the EOMs, it is sufficient to minimize the energy functional,

$$E = \int d^3x \mathcal{E} \quad (9)$$

with

$$\begin{aligned} \mathcal{E} = & (D_i \phi_1)^2 + (D_i \phi_2)^2 + V(\phi_1, \phi_2) + \frac{1}{2} (\partial_i A_j)^2 \\ & - \frac{1}{2} (\partial_i A_0)^2 - g A_0 J_0 + C \epsilon^{ijk} \partial_i a A_0 \partial_j A_k \\ & + \frac{\gamma - 1}{2} (\partial_i A_i)^2, \end{aligned} \quad (10)$$

and

$$J_0 \equiv g A_0 (q_1^2 |\phi_1|^2 + q_2^2 |\phi_2|^2), \quad (11)$$

where we have added the gauge fixing term $\gamma(\partial_i A_i)^2/2$ to realize the Coulomb gauge $\partial_i A_i = 0$ and γ is the gauge fixing parameter.

We here meet two obstructions to perform the minimization.

- The energy density (10) is apparently not positive definite because the temporal component A_0 has the “wrong sign”.
- For large C , the first-order differential term $A_0 \partial_j A_k$ is dominant over the kinetic term $(\partial_i A_j)^2$.

Due to the first obstruction, a naive minimization with respect to A_0 does not converge. To avoid this, we solve separately the EOM of A_0 called the Gauss-law constraint,

$$0 = \frac{\delta E}{\delta A_0} = \partial^2 A_0 - 2gJ_0 + C\epsilon^{ijk}\partial_i a \partial_j A_k, \quad (12)$$

from which it follows that Eq. (10) is rewritten as

$$\begin{aligned} \mathcal{E} = & (D_i \phi_1)^2 + (D_i \phi_2)^2 + V(\phi_1, \phi_2) + \frac{1}{2}(\partial_i A_j)^2 \\ & + \frac{1}{2}C\rho A_0 + \frac{\gamma-1}{2}(\partial_i A_i)^2 \end{aligned} \quad (13)$$

with $\rho = \epsilon^{ijk}(\partial_i a)\partial_j A_k$.¹⁴

The second point often produces a numerical instability when we discretize the system. To resolve this, we introduce an auxiliary field B_i and replace ρ as

$$\rho \rightarrow B_i \partial_i a \quad (14)$$

in Eq. (13) imposing constraints

$$B^i = \epsilon^{ijk}\partial_j A_k \quad (i = 1, 2, 3). \quad (15)$$

Thanks to this, there is no first-order differential term apparently. In order to realize these constraints, we follow the procedure presented in Ref. [118]. We introduce multiplier fields $w_i(x)$ and add terms

$$w_i(B^i - \epsilon^{ijk}\partial_j A_k) + \frac{U}{2}(B^i - \epsilon^{ijk}\partial_j A_k)^2 \quad (16)$$

to the energy density ($U = \text{const.}$). It is shown in Ref. [118] that these constraints are achieved by updating w_i iteratively as follows

$$w_i \rightarrow w_i + U(B^i - \epsilon^{ijk}\partial_j A_k) \quad (17)$$

¹⁴ This expression can be made obviously positive definite when one uses the following formal solution of the Gauss law,

$$A_0 = C[-\partial_i^2 + 2g^2(q_1^2|\phi_2|^2 + q_2^2|\phi_1|^2)]^{-1}\epsilon^{ijk}\partial_i a \partial_j A_k,$$

from which the fifth term in Eq. (13) becomes

$$\frac{C^2}{2}\rho[-\partial_i^2 + 2g^2(q_1^2|\phi_2|^2 + q_2^2|\phi_1|^2)]^{-1}\rho.$$

when U is sufficiently large.

Then the task is to minimize the three-dimensional integration of Eq. (13) in which A_0 is determined by solving the Gauss law constraint (12) and the constraints (15) are imposed. We introduce a naive spatial discretization with lattice spacing d and approximate the derivatives by second-order central-difference scheme. Denoting the all variables on the lattice sites by $u_{a,j} = \{\text{Re } \phi_{1,2}(x_j), \text{Im } \phi_{1,2}(x_j), A_i(x_j), B_i(x_j)\}$ and $s_j = A_0(x_j)$, we have $E \simeq d^3 \sum \mathcal{E}_{\text{disc}}(u_{a,j}, s_j)$, where the summation is taken over all lattice points.

We adopt the so-called relaxation procedure, in which one starts from appropriate values $u_a^{(0)}$ and solve an iterative equation,

$$u_{a,j}^{(n+1)} = u_{a,j}^{(n)} - \alpha \frac{\partial \mathcal{E}_{\text{disc}}(u^{(n)}, s^{(n)})}{\partial u_{a,j}^{(n)}}, \quad (18)$$

to obtain $(n+1)$ -th step values from n -th step ones. Here, α is the step size. To determine $s_j^{(n+1)}$, we solve the Gauss law numerically at each step by the similar procedure,

$$\begin{aligned} s_j^{(n+1)} = & s_j^{(n)} \\ & + \beta \left[\Delta s_j^{(n)} - 2gJ_0(u_{a,j}^{(n+1)}, s_j^{(n)}) + C\rho(u_{a,j}^{(n+1)}, s_j^{(n)}) \right] \end{aligned} \quad (19)$$

where Δ is the discretized Laplacian and β is the step size for s_j . In addition, we have to repeat the update for the multiplier w_i given by Eq. (17). To summarize, we repeat the following procedure:

$$[(18) \rightarrow (19) \rightarrow (17)] \rightarrow [(18) \rightarrow (19) \rightarrow (17)] \rightarrow \dots$$

If this iteration converges, the configuration is the static solution of the EOM with the conditions (12) and (15).

In this work, we take $\gamma = 1 + U$, $U = 50$, $d = 0.8/v$, $\alpha = 4 \times 10^{-4}v^{-2}$, and $\beta = 2 \times 10^{-3}v^{-2}$. The number of lattice sites is 320^3 . We use a convergence criteria that

$$\sum_a \overline{\left(u_{a,j}^{(n+1)} - u_{a,j}^{(n)} \right)^2} < 1.06 \times 320^{-3}, \quad (20)$$

where the overline indicates the spatial average.

B. Calculation of non-thermal leptogenesis

We here give more detailed calculation for leptogenesis from the knot decay. After N_1 's are produced from the knots, they further decay into H (H^\dagger) and ℓ ($\bar{\ell}$). It is convenient to introduce the so-called lepton asymmetry parameter defined through decay rates of the processes as

$$\epsilon \equiv \frac{\Gamma(N_1 \rightarrow H + \ell) - \Gamma(N_1 \rightarrow H^\dagger + \bar{\ell})}{\Gamma(N_1 \rightarrow H + \ell) + \Gamma(N_1 \rightarrow H^\dagger + \bar{\ell})}, \quad (21)$$

which depends on parameters of the model. Then, the produced lepton asymmetry per knot soliton is expressed as $\epsilon f_{N_1} M/M_{R1}$.

Since T_{rh} is assumed to be larger than the EW scale, the EW sphaleron process is equilibrated and convert the lepton number into the baryon number as

$$\begin{aligned} Y_B &= - \frac{28}{79} \frac{n_L - n_{\bar{L}}}{s} \Big|_{\text{decay}} \\ &\simeq - \frac{28}{79} \frac{\epsilon f_{N_1} n_{\text{knot}} M}{M_{R1}} \frac{45}{2\pi} \frac{1}{g_s T_{rh}^3} \Big|_{\text{decay}} \\ &\simeq - \frac{21\pi}{79} \epsilon f_{N_1} \frac{T_{rh}}{M_{R1}}, \end{aligned} \quad (22)$$

where $g_s (\simeq g_*)$ is the effective relativistic degrees of freedom for entropy. Note that M_{R1} should satisfy $M_{R1} > T_{rh}$ to avoid the wash-out effect.

When the masses M_{R1}, M_{R2}, M_{R3} are not degenerated, the parameter ϵ is maximized for a hierarchical case $M_{R1} \ll M_{R2}, M_{R3}$, as given by [112–115]

$$\epsilon \simeq - \frac{3}{8\pi} \frac{M_{R1}}{\langle H \rangle^2} m_3 \delta_{\text{eff}}. \quad (23)$$

Substituting Eq. (23) into Eq. (22), one gets Eq. (7).

On the other hand, when the masses of N_1 and N_2 are almost degenerated, ϵ can be enhanced to be as large as $\mathcal{O}(1)$ like resonant leptogenesis [116, 117]. In such a case, Y_B is given by Eq. (8).

C. Baryogenesis via linking flux

We present an alternative scenario that the knot decay may produce baryon asymmetry in the Universe even when T_{rh} is smaller than the EW scale $\mathcal{O}(10^2)$ GeV. The key is the fact that the ϕ_2 string also has the magnetic flux of the $U(1)_{B-L}$ gauge field and becomes a fractional vortex when ϕ_2 has a non-zero $B-L$ charge, $q_2 \neq 0$. This allows the knot solitons to have the linking magnetic fluxes of the $U(1)_{B-L}$ gauge field. This linking flux has the Chern-Simons number (or helicity) $N_{CS}[A] \sim q_1 q_2 N_{\text{link}}$.

In general, this $U(1)_{B-L}$ gauge field A_μ has a kinetic mixing with the $U(1)_Y$ gauge field in the SM, $\mathcal{L}_{\text{mix}} = (\epsilon_{\text{mix}}/2) F_{\mu\nu} Y^{\mu\nu}$, especially when they arise from a unified simple gauge group such as $SO(10)$. Due to the kinetic mixing, the magnetic flux of A_μ induces the flux of Y_μ along the ϕ_1 and ϕ_2 strings. Therefore a knot soliton with the Chern-Simons number of $U(1)_X$ must contain the Chern-Simons number of $U(1)_Y$, $N_{CS}[Y] \sim \epsilon_{\text{mix}}^2 N_{CS}[A] \sim \epsilon_{\text{mix}}^2 q_1 q_2 N_{\text{link}}$. In the broken phase of the EW symmetry, the $U(1)_Y$ flux is dressed as the Z boson flux [119], which is a superposition of the $U(1)_Y$ and $SU(2)_W$ fluxes. (The unbroken $U(1)$ electromagnetic flux is not induced.)

When the knots decay at cosmic time $t \simeq \tau_{\text{decay}}$, all the magnetic fluxes contained in the knots disappear, and hence $N_{CS}[Y]$ changes from $\epsilon_{\text{mix}}^2 q_1 q_2 N_{\text{link}}$ into

0 per knot. This decay process produces the baryon number because the baryon number is not conserved due to the quantum anomaly but is related with the change of the Chern-Simons number of the $U(1)_Y$ field as $\Delta B = 3\Delta N_{CS}[Y]$. Through this anomaly relation, the decay of each knot produces the baryon number $\Delta B \simeq \epsilon_{\text{mix}}^2 q_1 q_2 N_{\text{link}}$. Therefore the linking number of the knot solitons can be a seed of the baryon number without leptogenesis.

In Refs. [120, 121], baryogenesis is realized via decay of helical $U(1)_Y$ magnetic fields. While in their scenario the baryon number is produced during the EW phase transition (crossover), we now consider the case that the baryon number is produced after completion of the EW phase transition since T_{rh} is lower than the EW scale, and hence it is not washed out by the sphaleron process.

In this scenario, we should consider carefully the creation of the knot solitons. Indeed, when the knot solitons are produced by the Kibble-Zurek mechanism, anti-knot solitons, in which the ϕ_1 and ϕ_2 strings are linked with the relatively opposite direction compared to knot solitons, are necessarily produced as well. This anti-knot has the Chern-Simons number with the opposite sign, $N_{CS}[A] \sim -\epsilon_{\text{mix}}^2 q_1 q_2 N_{\text{link}}$. If there is no probability bias between the knots and anti-knots, their produced number should be equal, which results in that the net Chern-Simons number and hence the net baryon number are zero in total. To avoid this, one needs an effective chemical potential μ_{eff} between them around the phase transition $T \sim T_c$. We assume that the asymmetry between them is given by the Boltzmann factor, leading to

$$n_{\text{knot}} - \bar{n}_{\text{knot}} \Big|_{\text{production}} \sim n_{\text{knot}} \frac{\mu_{\text{eff}}(T_c)}{T_c} \quad (24)$$

within the linear perturbation assuming $\mu_{\text{eff}}(T_c)/T_c \lesssim 1$.

Using this, the produced net baryon number from the decay of the (anti)knots is given as (assuming $N_{\text{link}} \sim 1$)

$$\begin{aligned} Y_B &\sim \frac{n_{\text{knot}} - \bar{n}_{\text{knot}}}{s} \Big|_{\text{decay}} \epsilon_{\text{mix}}^2 q_1 q_2 \\ &\sim n_{\text{knot}} \Big|_{\text{decay}} \frac{\mu_{\text{eff}}(T_c)}{T_c} \epsilon_{\text{mix}}^2 q_1 q_2 \frac{45}{2\pi} \frac{1}{g_s T_{rh}^3} \\ &\sim 10^{-10} \frac{\mu_{\text{eff}}(T_c)}{T_c} \epsilon_{\text{mix}}^2 q_1 q_2 \left(\frac{T_{rh}}{100 \text{ GeV}} \right) \left(\frac{10^{12} \text{ GeV}}{M} \right). \end{aligned} \quad (25)$$

To get the observed baryon asymmetry, we need the mass of the knot soliton M smaller than 10^{12} GeV. However, M is typically given as $M \sim \mathcal{O}(10^3) v/g$, and v should satisfy $v \gtrsim 10^8$ GeV, in which the last inequality comes from astrophysical constraints on the axion decay constant, $f_a \gtrsim \mathcal{O}(10^8)$ GeV [85–88]. Thus successful baryogenesis works for 10^8 GeV $\lesssim v \lesssim 10^9$ GeV.

We here comment on two possible origins of the chemical potential μ_{eff} . The first one is a new pseudo scalar a' that behaves as a time-dependent background. If A_μ couples to a' via $a' F_{\mu\nu} \tilde{F}^{\mu\nu}$ in the Lagrangian, that term

becomes $\partial_t a' \epsilon^{ijk} A_i \partial_j A_k$, leading to $\mu_{\text{eff}} \simeq \partial_t a' N_{CS}[A]$. This resembles the Affleck-Dine mechanism [122], Axionogenesis [123], and the production of helical magnetic fields from axion inflation [124–126].

The second example of the chemical potential μ_{eff} is the chiral charge asymmetry n_5 , which can be produced from decays of heavy particles. For instance, the chiral charge of electrons can be produced [127, 128] in a similar way to the GUT baryogenesis [129–131] and is not washed out by the electron Yukawa coupling at high temperature. Through the chiral anomaly, this chiral asymmetry lowers (raises) energy of a helical (anti-helical) configuration of the $U(1)_Y$ gauge field, like chiral plasma instability [132]. Thus, an imbalance between the knot and anti-knot might be induced as $\mu_{\text{eff}} \simeq \mu_5 N_{CS}[Y]$ with $\mu_5 \sim n_5/T^2$.

In any case, we need some mechanism to give non-zero μ_{eff} that leads to an asymmetry between knots and anti-knots. Obviously, it is required to have a closer look at the Kibble-Zurek mechanism in the presence of μ_{eff} in order to obtain precise predictions of the asymmetry. After they are asymmetrically produced by the mechanism, the asymmetry is stored in the (anti-)knots as the net Chern-Simons number $N_{CS}[Y]$, and is converted into the baryon asymmetry by their decay. In this sense, the baryon asymmetry is “hidden” in the knot sector until the decay, and is eventually “released” into the Universe.

D. Calculation of gravitational wave spectrum

We present formulae to calculate the GW spectrum from a cosmic string network. For more details, see Refs. [96–98]. We assume that the network immediately approaches the scaling regime. The strings in the network move as Brownian motion and produce string loops by the reconnection. We model this in terms of velocity-dependent one-scale model [133–135] with a loop chopping efficiency $\bar{c} = 0.23$. Then, the produced number density of the loops per time at cosmic time t_i is given by

$$\frac{dn_{\text{loop}}}{dt_i} = C_{\text{eff}}(t_i) t_i^{-4}, \quad (26)$$

with an initial length $l = \alpha t_i$. We take $\alpha \simeq 0.1$ and $C_{\text{eff}}(t_i) = 0.41$ (5.5) for the matter dominated (radiation

dominated) Universe.

After the production, the loops oscillate and shrink by emitting GW. The length at time t is given as

$$l = \alpha t_i - \Gamma G \mu (t - t_i) \quad (27)$$

with the dimensionless constant $\Gamma \simeq 50$ [136–140]. Each oscillation mode k radiates GW with the frequency $f_{\text{emit}} = 2k/l$ ($k = 1, 2, \dots$). After emission at time \tilde{t} , the frequency redshifts due to the cosmic expansion until today as

$$f = \frac{a(\tilde{t})}{a(t_0)} \frac{2k}{l(\tilde{t})} = \frac{a(\tilde{t})}{a(t_0)} \frac{2k}{\alpha t_i - \Gamma G \mu (\tilde{t} - t_i)}, \quad (28)$$

where t_0 is the current time.

Summing over all oscillation modes, the energy density of GW per unit frequency observed today is given as

$$\Omega_{\text{GW}}(f) = \frac{f}{\rho_c} \frac{d\rho_{\text{GW}}}{df} = \sum_k \Omega_{\text{GW}}^{(k)}(f) \quad (29)$$

with

$$\begin{aligned} \Omega_{\text{GW}}^{(k)}(f) &= \frac{1}{\rho_c} \frac{2k}{f} \frac{\Gamma_k G \mu^2}{\alpha + \Gamma G \mu} \\ &\times \int_{t_F}^{t_0} d\tilde{t} \frac{C_{\text{eff}}(t_i)}{t_i^4} \left(\frac{a(\tilde{t})}{a(t_0)} \right)^5 \left(\frac{a(t_i)}{a(\tilde{t})} \right)^3 \Theta(t_i - t_F), \end{aligned} \quad (30)$$

where $\rho_c = 3H_0^2/8\pi G$ is the critical density and $\Gamma_k = \Gamma k^{-4/3}/3.6$ [139, 140]. t_F is the formation time of the string network, which can be taken to be 0 essentially. We assume that the GW emission is dominated by cusps. The relation between \tilde{t} and t_i is given by Eq. (28). Θ is the Heaviside step function.

We assume sudden transitions between the radiation dominated and knot dominated eras. The summation over the modes k is performed by the method presented in Ref. [141], to be taken up to $k_{\text{max}} = 10^{12}$, which gives the slopes $f^{-1/3}$ [141, 142] at higher frequency regime of the spectra with the knot dominated era. Although one may truncate the summation within smaller values, it affects only an asymptotic behavior at high frequency. Fig. 4 is obtained by plotting Eq. (29) utilizing these techniques.

[1] W. H. Thomson, *On Vortex Motion*, *Trans. R. Soc. Edin.* **25** (1869) 217.
 [2] P. G. Tait, *On knots i, ii, iii*, *Scientific papers* **1** (1898) 273.
 [3] L. H. Kauffman, *Knots and physics*, Series on Knots & Everything. World Scientific Publishing Co Pte Ltd, 1991, 10.1142/4256.
 [4] L. D. Faddeev and A. J. Niemi, *Knots and particles*,

Nature **387** (1997) 58 [[hep-th/9610193](#)].
 [5] H. K. Moffatt, *The degree of knottedness of tangled vortex lines*, *Journal of Fluid Mechanics* **35** (1969) 117–129.
 [6] R. L. Ricca and M. A. Berger, *Topological Ideas and Fluid Mechanics*, *Physics Today* **49** (1996) 28.
 [7] R. L. Ricca, *New developments in topological fluid mechanics*, *Nuovo Cim.* **C 32** (2009) 185.

- [8] D. Kleckner and W. T. M. Irvine, *Creation and dynamics of knotted vortices*, *Nature Physics* **9** (2013) 253.
- [9] V. I. Arnold and B. A. Khesin, *Topological Methods in Hydrodynamics*. Springer Cham, 2021, 10.1007/978-3-030-74278-2.
- [10] E. Babaev, L. D. Faddeev and A. J. Niemi, *Hidden symmetry and knot solitons in a charged two-condensate Bose system*, *Phys. Rev. B* **65** (2002) 100512 [[cond-mat/0106152](#)].
- [11] F. N. Rybakov, J. Garaud and E. Babaev, *Stable Hopf-Skyrme topological excitations in the superconducting state*, *Phys. Rev. B* **100** (2019) 094515 [[1807.02509](#)].
- [12] D. Proment, M. Onorato and C. F. Barenghi, *Vortex knots in a bose-einstein condensate*, *Phys. Rev. E* **85** (2012) 036306.
- [13] D. Kleckner, L. H. Kauffman and W. T. M. Irvine, *How superfluid vortex knots untie*, *Nature Physics* (2016) 650–655.
- [14] Y. Kawaguchi, M. Nitta and M. Ueda, *Knots in a Spinor Bose-Einstein Condensate*, *Phys. Rev. Lett.* **100** (2008) 180403 [[0802.1968](#)].
- [15] D. Hall, M. Ray and K. Tiurev *et.al.*, *Tying quantum knots*, *Nature Phys* **12** (2016) 478.
- [16] T. Ollikainen, A. Blinova, M. Möttönen and D. S. Hall, *Decay of a Quantum Knot*, *Phys. Rev. Lett.* **123** (2019) 163003 [[1908.01285](#)].
- [17] G. Volovik and V.P.Mineev, *Particle-like solitons in superfluid 3he phases*, *JETP* **46** (1977) 401.
- [18] G. E. Volovik, *The Universe in a helium droplet*, International Series of Monographs on Physics. Oxford Scholarship Online, 2009, 10.1093/acprof:oso/9780199564842.001.0001.
- [19] B. G.-g. Chen, P. J. Ackerman, G. P. Alexander, R. D. Kamien and I. I. Smalyukh, *Generating the hopf fibration experimentally in nematic liquid crystals*, *Phys. Rev. Lett.* **110** (2013) 237801.
- [20] T. Machon and G. P. Alexander, *Knotted defects in nematic liquid crystals*, *Phys. Rev. Lett.* **113** (2014) 027801.
- [21] P. Ackerman, J. van de Lagemaat and I. Smalyukh, *Self-assembly and electrostriction of arrays and chains of hopfion particles in chiral liquid crystals*, *Nat. Comm.* **6** (2015) 6012.
- [22] P. Ackerman and I. Smalyukh, *Static three-dimensional topological solitons in fluid chiral ferromagnets and colloids*, *Nat. Mater.* **16** (2017) 426.
- [23] P. Ackerman and I. Smalyukh, *Diversity of knot solitons in liquid crystals manifested by linking of preimages in torons and hopfions*, *Phys. Rev. X* **7** (2017) 011006.
- [24] J.-S. Tai, P. Ackerman and I. Smalyukh, *Topological transformations of hopf solitons in chiral ferromagnets and liquid crystals*, *PNAS* **115** (2018) 921.
- [25] J.-S. B. Tai and I. I. Smalyukh, *Three-dimensional crystals of adaptive knots*, *Science* **365** (2019) 1449–1453.
- [26] G. P. Alexander, B. G.-g. Chen, E. A. Matsumoto and R. D. Kamien, *Colloquium: Disclination loops, point defects, and all that in nematic liquid crystals*, *Rev. Mod. Phys.* **84** (2012) 497.
- [27] I. I. Smalyukh, *Review: knots and other new topological effects in liquid crystals and colloids*, *Rept. Prog. Phys.* **83** (2020) 106601.
- [28] J.-S. Wu and I. I. Smalyukh, *Hopfions, heliknotons, skyrmions, torons and both abelian and nonabelian vortices in chiral liquid crystals*. Taylor & Francis, 2022, 10.1080/21680396.2022.2040058.
- [29] N. Kent et al., *Creation and observation of Hopfions in magnetic multilayer systems*, *Nature Commun.* **12** (2021) 1562 [[2010.08674](#)].
- [30] M. R. Dennis, R. P. King, B. Jack, K. O’Holleran and M. J. Padgett, *Isolated optical vortex knots*, *Nature Physics* **6** (2010) 118.
- [31] A. Trautman, *Solutions of the Maxwell and Yang-Mills Equations Associated with Hopf Fibrings*, *Int. J. Theor. Phys.* **16** (1977) 561.
- [32] A. F. Ranada, *A Topological Theory of the Electromagnetic Field*, *Lett. Math. Phys.* **18** (1989) 97.
- [33] H. Kedia, I. Bialynicki-Birula, D. Peralta-Salas and W. T. M. Irvine, *Tying knots in light fields*, *Phys. Rev. Lett.* **111** (2013) 150404 [[1302.0342](#)].
- [34] M. Arrayás, D. Bouwmeester and J. L. Trueba, *Knots in electromagnetism*, *Phys. Rept.* **667** (2017) 1.
- [35] S. Shankar, A. Souslov, M. J. Bowick, M. C. Marchetti and V. Vitelli, *Topological active matter*, *Nat Rev Phys* **4** (2022) 380.
- [36] E. Witten, *Quantum Field Theory and the Jones Polynomial*, *Commun. Math. Phys.* **121** (1989) 351.
- [37] R. A. Battye and P. M. Sutcliffe, *Knots as stable soliton solutions in a three-dimensional classical field theory.*, *Phys. Rev. Lett.* **81** (1998) 4798 [[hep-th/9808129](#)].
- [38] N. S. Manton and P. Sutcliffe, *Topological solitons*, Cambridge Monographs on Mathematical Physics. Cambridge University Press, 2004, 10.1017/CBO9780511617034.
- [39] E. Radu and M. S. Volkov, *Existence of stationary, non-radiating ring solitons in field theory: knots and vortons*, *Phys. Rept.* **468** (2008) 101 [[0804.1357](#)].
- [40] M. Kobayashi and M. Nitta, *Torus knots as Hopfions*, *Phys. Rev. Lett. B* **728** (2014) 314 [[1304.6021](#)].
- [41] Y. M. Shnir, *Topological and Non-Topological Solitons in Scalar Field Theories*. Cambridge University Press, 7, 2018, 10.1017/9781108555623.
- [42] E. Babaev, A. Sudbo and N. W. Ashcroft, *A Superconductor to superfluid phase transition in liquid metallic hydrogen*, *Nature* **431** (2004) 666 [[cond-mat/0410408](#)].
- [43] J. Smiseth, E. Smorgrav, E. Babaev and A. Sudbo, *Field and temperature induced topological phase transitions in the three-dimensional N-component London superconductor*, *Phys. Rev. B* **71** (2005) 214509 [[cond-mat/0411761](#)].
- [44] E. Babaev, *Andreev-Bashkin effect and knot solitons in neutron stars*, *Phys. Rev. D* **70** (2004) 043001 [[astro-ph/0211345](#)].
- [45] R. Peccei and H. R. Quinn, *CP Conservation in the Presence of Instantons*, *Phys. Rev. Lett.* **38** (1977) 1440.
- [46] R. Peccei and H. R. Quinn, *Constraints Imposed by CP Conservation in the Presence of Instantons*, *Phys. Rev. D* **16** (1977) 1791.
- [47] Y. Hidaka, M. Nitta and R. Yokokura, *Topological axion electrodynamics and 4-group symmetry*, *Phys. Rev. Lett. B* **823** (2021) 136762 [[2107.08753](#)].
- [48] Y. Hidaka, M. Nitta and R. Yokokura, *Global 4-group*

- symmetry and 't Hooft anomalies in topological axion electrodynamics*, *PTEP* **2022** (2022) 04A109 [2108.12564].
- [49] Y. Hidaka, M. Nitta and R. Yokokura, *Global 3-group symmetry and 't Hooft anomalies in axion electrodynamics*, *JHEP* **01** (2021) 173 [2009.14368].
- [50] Y. Hidaka, M. Nitta and R. Yokokura, *Higher-form symmetries and 3-group in axion electrodynamics*, *Phys. Lett. B* **808** (2020) 135672 [2006.12532].
- [51] F. Wilczek, *Two Applications of Axion Electrodynamics*, *Phys. Rev. Lett.* **58** (1987) 1799.
- [52] X.-L. Qi, E. Witten and S.-C. Zhang, *Axion topological field theory of topological superconductors*, *Phys. Rev. B* **87** (2013) 134519 [1206.1407].
- [53] M. Stone and P. L. S. Lopes, *Effective action and electromagnetic response of topological superconductors and Majorana-mass Weyl fermions*, *Phys. Rev. B* **93** (2016) 174501 [1601.07869].
- [54] M. Stålhammar, M. Stone, M. Sato and T. H. Hansson, *Electromagnetic response of topological superconductors*, *Phys. Rev. B* **103** (2021) 235427 [2103.08960].
- [55] P. A. Horvathy, *Lectures on (abelian) Chern-Simons vortices*, **4**, 2007, 0704.3220.
- [56] P. A. Horvathy and P. Zhang, *Vortices in (abelian) Chern-Simons gauge theory*, *Phys. Rept.* **481** (2009) 83 [0811.2094].
- [57] N. Yokoi, *Cross helicity and related dynamo*, *Geophysical and Astrophysical Fluid Dynamics* **107** (2013) 114–184.
- [58] H. Nastase and J. Sonnenschein, *Fluid-electromagnetic helicities and knotted solutions of the fluid-electromagnetic equations*, *JHEP* **12** (2022) 144 [2205.10415].
- [59] R. L. Davis and E. P. S. Shellard, *Cosmic Vortons*, *Nucl. Phys. B* **323** (1989) 209.
- [60] R. L. Davis and E. P. S. Shellard, *The Physics of Vortex Superconductivity. 2*, *Phys. Lett. B* **209** (1988) 485.
- [61] R. A. Battye and P. M. Sutcliffe, *Vorton construction and dynamics*, *Nucl. Phys. B* **814** (2009) 180 [0812.3239].
- [62] J. Garaud, E. Radu and M. S. Volkov, *Stable Cosmic Vortons*, *Phys. Rev. Lett.* **111** (2013) 171602 [1303.3044].
- [63] R. A. Battye and S. J. Cotterill, *Stable Cosmic Vortons in Bosonic Field Theory*, *Phys. Rev. Lett.* **127** (2021) 241601 [2111.07822].
- [64] R. A. Battye, S. J. Cotterill and J. A. Pearson, *A detailed study of the stability of vortons*, *JHEP* **04** (2022) 005 [2112.08066].
- [65] M. Ibe, S. Kobayashi, Y. Nakayama and S. Shirai, *On Stability of Fermionic Superconducting Current in Cosmic String*, *JHEP* **05** (2021) 217 [2102.05412].
- [66] Y. Abe, Y. Hamada, K. Saji and K. Yoshioka, *Quantum current dissipation in superconducting strings and vortons*, *JHEP* **02** (2023) 004 [2209.03223].
- [67] S. B. Gudnason and M. Nitta, *Linking number of vortices as baryon number*, *Phys. Rev. D* **101** (2020) 065011 [2002.01762].
- [68] S. B. Gudnason and M. Nitta, *Linked vortices as baryons in the miscible BEC-Skyrme model*, *Phys. Rev. D* **102** (2020) 045022 [2006.04067].
- [69] J. Ruostekoski and J. R. Anglin, *Creating vortex rings and three-dimensional skyrmions in Bose-Einstein condensates*, *Phys. Rev. Lett.* **86** (2001) 3934 [cond-mat/0103310].
- [70] R. A. Battye, N. R. Cooper and P. M. Sutcliffe, *Stable skyrmions in two component Bose-Einstein condensates*, *Phys. Rev. Lett.* **88** (2002) 080401 [cond-mat/0109448].
- [71] M. Nitta, K. Kasamatsu, M. Tsubota and H. Takeuchi, *Creating vortons and three-dimensional skyrmions from domain wall annihilation with stretched vortices in Bose-Einstein condensates*, *Phys. Rev. A* **85** (2012) 053639 [1203.4896].
- [72] M. Eto, K. Kasamatsu, M. Nitta, H. Takeuchi and M. Tsubota, *Interaction of half-quantized vortices in two-component Bose-Einstein condensates*, *Phys. Rev. A* **83** (2011) 063603 [1103.6144].
- [73] H. Ooguri and M. Oshikawa, *Instability in magnetic materials with dynamical axion field*, *Phys. Rev. Lett.* **108** (2012) 161803 [1112.1414].
- [74] PARTICLE DATA GROUP collaboration, *Review of Particle Physics*, *PTEP* **2022** (2022) 083C01.
- [75] S. Weinberg, *A New Light Boson?*, *Phys. Rev. Lett.* **40** (1978) 223.
- [76] F. Wilczek, *Problem of Strong P and T Invariance in the Presence of Instantons*, *Phys. Rev. Lett.* **40** (1978) 279.
- [77] P. Minkowski, *$\mu \rightarrow e\gamma$ at a Rate of One Out of 10^9 Muon Decays?*, *Phys. Lett. B* **67** (1977) 421.
- [78] M. Gell-Mann, P. Ramond and R. Slansky, *Complex Spinors and Unified Theories*, *Conf. Proc. C* **790927** (1979) 315 [1306.4669].
- [79] R. N. Mohapatra and G. Senjanovic, *Neutrino Mass and Spontaneous Parity Nonconservation*, *Phys. Rev. Lett.* **44** (1980) 912.
- [80] T. Yanagida, *Horizontal gauge symmetry and masses of neutrinos*, *Conf. Proc. C* **7902131** (1979) 95.
- [81] H. Fukuda, M. Ibe, M. Suzuki and T. T. Yanagida, *A "gauged" $U(1)$ Peccei-Quinn symmetry*, *Phys. Lett. B* **771** (2017) 327 [1703.01112].
- [82] M. Ibe, M. Suzuki and T. T. Yanagida, *$B - L$ as a Gauged Peccei-Quinn Symmetry*, *JHEP* **08** (2018) 049 [1805.10029].
- [83] J. E. Kim, *Weak Interaction Singlet and Strong CP Invariance*, *Phys. Rev. Lett.* **43** (1979) 103.
- [84] M. A. Shifman, A. Vainshtein and V. I. Zakharov, *Can Confinement Ensure Natural CP Invariance of Strong Interactions?*, *Nucl. Phys. B* **166** (1980) 493.
- [85] G. G. Raffelt, *Astrophysical axion bounds*, *Lect. Notes Phys.* **741** (2008) 51 [hep-ph/0611350].
- [86] I. G. Irastorza and J. Redondo, *New experimental approaches in the search for axion-like particles*, *Prog. Part. Nucl. Phys.* **102** (2018) 89 [1801.08127].
- [87] J. H. Chang, R. Essig and S. D. McDermott, *Supernova 1987A Constraints on Sub-GeV Dark Sectors, Millicharged Particles, the QCD Axion, and an Axion-like Particle*, *JHEP* **09** (2018) 051 [1803.00993].
- [88] K. Hamaguchi, N. Nagata, K. Yanagi and J. Zheng, *Limit on the Axion Decay Constant from the Cooling Neutron Star in Cassiopeia A*, *Phys. Rev. D* **98** (2018) 103015 [1806.07151].
- [89] T. W. B. Kibble, *Some Implications of a Cosmological Phase Transition*, *Phys. Rept.* **67** (1980) 183.
- [90] W. H. Zurek, *Cosmological Experiments in Superfluid*

- Helium?*, *Nature* **317** (1985) 505.
- [91] T. Vachaspati and G. B. Field, *Electroweak string configurations with baryon number*, *Phys. Rev. Lett.* **73** (1994) 373 [[hep-ph/9401220](#)].
- [92] E. W. Kolb and M. S. Turner, *The Early Universe*, vol. 69. 1990, 10.1201/9780429492860.
- [93] M. Kawasaki, K. Kohri and N. Sugiyama, *Cosmological constraints on late time entropy production*, *Phys. Rev. Lett.* **82** (1999) 4168 [[astro-ph/9811437](#)].
- [94] M. Kawasaki, K. Kohri and N. Sugiyama, *MeV scale reheating temperature and thermalization of neutrino background*, *Phys. Rev. D* **62** (2000) 023506 [[astro-ph/0002127](#)].
- [95] S. Hannestad, *What is the lowest possible reheating temperature?*, *Phys. Rev. D* **70** (2004) 043506 [[astro-ph/0403291](#)].
- [96] Y. Cui, M. Lewicki, D. E. Morrissey and J. D. Wells, *Cosmic Archaeology with Gravitational Waves from Cosmic Strings*, *Phys. Rev. D* **97** (2018) 123505 [[1711.03104](#)].
- [97] Y. Cui, M. Lewicki, D. E. Morrissey and J. D. Wells, *Probing the pre-BBN universe with gravitational waves from cosmic strings*, *JHEP* **01** (2019) 081 [[1808.08968](#)].
- [98] Y. Gouttenoire, G. Servant and P. Simakachorn, *Beyond the Standard Models with Cosmic Strings*, *JCAP* **07** (2020) 032 [[1912.02569](#)].
- [99] NANOGrav collaboration, *The NANOGrav 15 yr Data Set: Evidence for a Gravitational-wave Background*, *Astrophys. J. Lett.* **951** (2023) L8 [[2306.16213](#)].
- [100] NANOGrav collaboration, *The NANOGrav 15 yr Data Set: Search for Signals from New Physics*, *Astrophys. J. Lett.* **951** (2023) L11 [[2306.16219](#)].
- [101] K. Schmitz, *New Sensitivity Curves for Gravitational-Wave Signals from Cosmological Phase Transitions*, *JHEP* **01** (2021) 097 [[2002.04615](#)].
- [102] S. Kawamura et al., *Current status of space gravitational wave antenna DECIGO and B-DECIGO*, *PTEP* **2021** (2021) 05A105 [[2006.13545](#)].
- [103] D. Reitze et al., *Cosmic Explorer: The U.S. Contribution to Gravitational-Wave Astronomy beyond LIGO*, *Bull. Am. Astron. Soc.* **51** (2019) 035 [[1907.04833](#)].
- [104] N. Bartolo et al., *Science with the space-based interferometer LISA. IV: Probing inflation with gravitational waves*, *JCAP* **12** (2016) 026 [[1610.06481](#)].
- [105] G. Janssen et al., *Gravitational wave astronomy with the SKA*, *PoS AASKA14* (2015) 037 [[1501.00127](#)].
- [106] PLANCK collaboration, *Planck 2018 results. VI. Cosmological parameters*, *Astron. Astrophys.* **641** (2020) A6 [[1807.06209](#)].
- [107] T. Asaka, K. Hamaguchi, M. Kawasaki and T. Yanagida, *Leptogenesis in inflaton decay*, *Phys. Lett. B* **464** (1999) 12 [[hep-ph/9906366](#)].
- [108] G. F. Giudice, M. Peloso, A. Riotto and I. Tkachev, *Production of massive fermions at preheating and leptogenesis*, *JHEP* **08** (1999) 014 [[hep-ph/9905242](#)].
- [109] T. Asaka, K. Hamaguchi, M. Kawasaki and T. Yanagida, *Leptogenesis in inflationary universe*, *Phys. Rev. D* **61** (2000) 083512 [[hep-ph/9907559](#)].
- [110] G. Lazarides and Q. Shafi, *Origin of matter in the inflationary cosmology*, *Phys. Lett. B* **258** (1991) 305.
- [111] K. Kumekawa, T. Moroi and T. Yanagida, *Flat potential for inflaton with a discrete R invariance in supergravity*, *Prog. Theor. Phys.* **92** (1994) 437 [[hep-ph/9405337](#)].
- [112] M. Flanz, E. A. Paschos and U. Sarkar, *Baryogenesis from a lepton asymmetric universe*, *Phys. Lett. B* **345** (1995) 248 [[hep-ph/9411366](#)].
- [113] L. Covi, E. Roulet and F. Vissani, *CP violating decays in leptogenesis scenarios*, *Phys. Lett. B* **384** (1996) 169 [[hep-ph/9605319](#)].
- [114] W. Buchmuller and M. Plumacher, *CP asymmetry in Majorana neutrino decays*, *Phys. Lett. B* **431** (1998) 354 [[hep-ph/9710460](#)].
- [115] S. Davidson and A. Ibarra, *A Lower bound on the right-handed neutrino mass from leptogenesis*, *Phys. Lett. B* **535** (2002) 25 [[hep-ph/0202239](#)].
- [116] A. Pilaftsis, *CP violation and baryogenesis due to heavy Majorana neutrinos*, *Phys. Rev. D* **56** (1997) 5431 [[hep-ph/9707235](#)].
- [117] A. Pilaftsis and T. E. J. Underwood, *Resonant leptogenesis*, *Nucl. Phys. B* **692** (2004) 303 [[hep-ph/0309342](#)].
- [118] M. R. Hestenes, *Multiplier and gradient methods*, *Journal of Optimization Theory and Applications* **4** (1969) 303.
- [119] J. M. Hyde, A. J. Long and T. Vachaspati, *Dark Strings and their Couplings to the Standard Model*, *Phys. Rev. D* **89** (2014) 065031 [[1312.4573](#)].
- [120] K. Kamada and A. J. Long, *Baryogenesis from decaying magnetic helicity*, *Phys. Rev. D* **94** (2016) 063501 [[1606.08891](#)].
- [121] K. Kamada and A. J. Long, *Evolution of the Baryon Asymmetry through the Electroweak Crossover in the Presence of a Helical Magnetic Field*, *Phys. Rev. D* **94** (2016) 123509 [[1610.03074](#)].
- [122] I. Affleck and M. Dine, *A New Mechanism for Baryogenesis*, *Nucl. Phys. B* **249** (1985) 361.
- [123] R. T. Co and K. Harigaya, *Axiogenesis*, *Phys. Rev. Lett.* **124** (2020) 111602 [[1910.02080](#)].
- [124] M. S. Turner and L. M. Widrow, *Inflation Produced, Large Scale Magnetic Fields*, *Phys. Rev. D* **37** (1988) 2743.
- [125] W. D. Garretson, G. B. Field and S. M. Carroll, *Primordial magnetic fields from pseudoGoldstone bosons*, *Phys. Rev. D* **46** (1992) 5346 [[hep-ph/9209238](#)].
- [126] M. M. Anber and L. Sorbo, *N-flationary magnetic fields*, *JCAP* **10** (2006) 018 [[astro-ph/0606534](#)].
- [127] K. Kamada, *Return of grand unified theory baryogenesis: Source of helical hypermagnetic fields for the baryon asymmetry of the universe*, *Phys. Rev. D* **97** (2018) 103506 [[1802.03055](#)].
- [128] V. Domcke, K. Kamada, K. Mukaida, K. Schmitz and M. Yamada, *Wash-In Leptogenesis*, *Phys. Rev. Lett.* **126** (2021) 201802 [[2011.09347](#)].
- [129] M. Yoshimura, *Unified Gauge Theories and the Baryon Number of the Universe*, *Phys. Rev. Lett.* **41** (1978) 281.
- [130] A. Y. Ignatiev, N. V. Krasnikov, V. A. Kuzmin and A. N. Tavkhelidze, *Universal CP Noninvariant Superweak Interaction and Baryon Asymmetry of the Universe*, *Phys. Lett. B* **76** (1978) 436.
- [131] S. Weinberg, *Cosmological Production of Baryons*, *Phys. Rev. Lett.* **42** (1979) 850.

- [132] Y. Akamatsu and N. Yamamoto, *Chiral Plasma Instabilities*, *Phys. Rev. Lett.* **111** (2013) 052002 [1302.2125].
- [133] C. J. A. P. Martins and E. P. S. Shellard, *String evolution with friction*, *Phys. Rev. D* **53** (1996) 575 [hep-ph/9507335].
- [134] C. J. A. P. Martins and E. P. S. Shellard, *Quantitative string evolution*, *Phys. Rev. D* **54** (1996) 2535 [hep-ph/9602271].
- [135] C. J. A. P. Martins and E. P. S. Shellard, *Extending the velocity dependent one scale string evolution model*, *Phys. Rev. D* **65** (2002) 043514 [hep-ph/0003298].
- [136] A. Vilenkin, *Gravitational radiation from cosmic strings*, *Phys. Lett. B* **107** (1981) 47.
- [137] N. Turok, *Grand Unified Strings and Galaxy Formation*, *Nucl. Phys. B* **242** (1984) 520.
- [138] J. M. Quashnock and D. N. Spergel, *Gravitational Selfinteractions of Cosmic Strings*, *Phys. Rev. D* **42** (1990) 2505.
- [139] J. J. Blanco-Pillado, K. D. Olum and B. Shlaer, *The number of cosmic string loops*, *Phys. Rev. D* **89** (2014) 023512 [1309.6637].
- [140] J. J. Blanco-Pillado and K. D. Olum, *Stochastic gravitational wave background from smoothed cosmic string loops*, *Phys. Rev. D* **96** (2017) 104046 [1709.02693].
- [141] S. Blasi, V. Brdar and K. Schmitz, *Has NANOGrav found first evidence for cosmic strings?*, *Phys. Rev. Lett.* **126** (2021) 041305 [2009.06607].
- [142] S. Blasi, V. Brdar and K. Schmitz, *Fingerprint of low-scale leptogenesis in the primordial gravitational-wave spectrum*, *Phys. Rev. Res.* **2** (2020) 043321 [2004.02889].